Cryobiology 89 (2019) 26–34

Contents lists available at ScienceDirect

Cryobiology

journal homepage: www.elsevier.com/locate/cryo

On the assessment of the stability of vitrified cryo-media by differential scanning calorimetry: A new tool for biobanks to derive standard operating procedures for storage, access and transport

Asger Kreiner[a], Frank Stracke[a], Heiko Zimmermann[a,b,c,*]

[a] Fraunhofer Institute for Biomedical Engineering, 66280, Sulzbach, Germany
[b] Department of Molecular and Cellular Biotechnology, Saarland University, 66123, Saarbrücken, Germany
[c] Faculty of Marine Science, Universidad Católica del Norte, Coquimbo, Chile

ARTICLE INFO

Keywords:
Devitrification
Glass stability
Johnson-Mehl-Avrami-Kolmogorov model
Differential scanning calorimetry
Dimethylsulfoxide
Ethylene glycol
Vitrification
Cryopreservation

ABSTRACT

When a vitrified sample is heated over the glass transition temperature it may start to devitrify endangering the sample. The ability to estimate the stability of the vitrified state can help in the development of new vitrification media as well as handling procedures. By employing differential scanning calorimetry, we can measure the ice crystallization rate in a vitrified sample and thus study the devitrification kinetics. Using this technique, we have studied samples comprised of PBS with cryoprotective additives (CPA) as dimethylsulfoxide (Me_2SO), ethylene glycol (EG) and mixtures thereof, regarding the dependence of the devitrification kinetics on the CPA concentration. We found that already small concentration changes lead to significant changes in the devitrification times. Changing the CPA concentration by 4 wt% changed the devitrification time with a factor of 342 and 271 for Me_2SO and EG, respectively. Concentration changes in EG/Me_2SO mixtures was found to have a smaller impact on the devitrification kinetics compared to the pure CPA samples. Our data suggest that these significant increases in the devitrification times are primarily due to a relation between nucleation rates and the CPA concentration. Finally, we investigated an established vitrification medium used to preserve human embryonic stem cells. This medium was found to have the poorest glass stability in this study and reflects the tradeoff between stability and biocompatibility. The present work finally provides a tool to evaluate handling and storage procedures when employing vitrification as a cryopreservation method and underlines the importance of these.

1. Introduction

Vitrification is an important method to preserve delicate biological material [11,28]. The approach relies on high concentrations of cryoprotective additives (CPA) and rapid cooling to well below the glass transition temperature T_g. The result hereof is that the sample is out of thermodynamic equilibrium and the liquid in the sample has therefore formed a glass. This is the main preserving feature of vitrification, since the biological material becomes immersed in a glass that effectively stops all biological and chemical processes. In contrast to the slow freezing approach, the biological molecules and structures remain in an almost natively hydrated state during vitrification, with no osmotic imbalances and segregation effects occurring.

One definition of the vitrified state is said to be when the viscosity of the liquid is higher than 10^{12} Pas [9], which happens below T_g. A sample will have to traverse a metastable region, where ice crystals possibly can nucleate and grow, in order to reach this stable region [23,39]. By cooling the sample sufficiently fast, ice crystallization can be avoided. There are several methods to achieve a vitrified state and common for these are that the sample volume is kept small and that high concentrations of CPAs are used. Using a small sample volume or having a thin sample [5,7,20,21,30,38] ensures that the cooling of the sample is not limited by the relatively low heat conductivity of water allowing for high cooling rates throughout the sample. High concentrations of CPAs reduce the cooling rate that is required to reach the vitrified state [36,39]. Very high cooling rates on the order of -10^7 K/s [37] are required for vitrification of pure water, which is impossible for volumes required for bio-specimens [42].

If a sample is heated above T_g after successful vitrification, the metastable region is entered again allowing ice crystals to nucleate and grow. This process is called devitrification and commonly known to be detrimental to cell viability [18,22]. Samples are conventionally stored in the vapor phase above a liquid nitrogen reservoir. The storage microenvironment is on occasion not well defined, controlled or monitored

* Corresponding author. Fraunhofer Institute for Biomedical Engineering, 66280, Sulzbach, Germany.
E-mail address: heiko.zimmermann@ibmt.fraunhofer.de (H. Zimmermann).

https://doi.org/10.1016/j.cryobiol.2019.06.002
Received 22 February 2019; Received in revised form 22 May 2019; Accepted 12 June 2019
Available online 13 June 2019

and it is possible that a sample can experience instances of elevated temperatures above T_g during its storage and handling [13]. Sample transport, extraction of a neighboring sample or sample handling in a cryo-workbench are instances where the sample temperature possibly could be raised above T_g. The risk of devitrification rises with higher temperatures as well as with the period of a given temperature elevation. Recent studies have shown that high warming rates are more important for a successful cryopreservation vitrification protocol than high cooling rates [24,33–35]. This underlines that even short temperature elevations poses a significant risk to vitrified samples and that stable storage conditions are critical. The stability of the vitrified state should also be considered when developing new cryopreservation protocols or media.

Devitrification is not an instantaneous process that happens as soon as a sample is elevated above T_g, but rather a time dependent process. Since the cooling rate required to reach the vitrified state depends highly on the chosen CPA and its concentration [36], it can be assumed that the time it takes for a given sample to devitrify is also dependent on the chemical composition of the vitrification medium. Many investigations have been performed in order to reveal the mechanisms determining the observed crystallization kinetics for different aqueous mixtures of CPAs [4,6,16,22,25,36]. From these results, minimum cooling and rewarming velocities can be estimated required to prevent significant ice formation for a given sample under ideal conditions. In this work, we focus on more application-oriented consequences of devitrification kinetics with respect to real-life biobank procedures and handling of vitrified samples. To this end PBS was used instead of ultrapure water as a mimic of osmotically balanced cell culture media and the additives were used as purchased without any purification steps. We excluded other typical cell culture additives like amino acids, proteins, sugars and so on from the samples in this study in order to avoid interactions between the compounds that may obscure the effects of Me_2SO and ethylene glycol on the devitrification tendency of the mixtures. Additionally, the results for these essential vitrification mixtures are compared to those of an established vitrification medium.

The aims of this study are outlined in the following:

- to investigate the concentration dependence of some common additives and their combination on devitrification rates
- to include an approved vitrification medium into the investigation and compare it with the model compositions
- to establish an experimental protocol for the estimation of maximum exposure times for vitrified media at given temperatures above T_g to set the base for handling procedures for vitrified samples

This work is supposed to help in the development of vitrification media and protocols that are less prone to unwanted and unforeseen temperature elevations and thus improve handling protocols for vitrified samples. Most other works in the field focus on determining the minimal cooling/heating rate required to successfully vitrify/rewarm a sample. In praxis yet, the highest possible cooling and heating rates are generally employed. In contrast, we will focus on how long a given sample can be kept safely at a given temperature in this study. The investigation is carried out by employing differential scanning calorimetry (DSC) on samples containing Me_2SO, EG and a 50 vol%/50 vol% mixture of EG/Me_2SO as well as an established vitrification medium (VS) used for the cryopreservation of human embryonic stem cells (hESC) [5,27,31]. DSC measures the heat released by crystallization of ice. This allows us to study the rate of isothermal ice crystallization over time and to determine the duration of the devitrification process, since the heat released is directly proportional to the ice crystallization rate. The devitrification process is analyzed using the Johnson-Mehl-Avrami-Kolmogorov (JMAK) model commonly used to analyze crystallization kinetics [12,15,22,25,40].

2. Materials and methods

2.1. Sample preparation

First, 45 µL of the given mixture was pipetted into an aluminum sample pan (PerkinElmer, US, part no. B016-9321, 50 µL) and the weight of the sample was recorded. The sample pan was then sealed with an aluminum lid using a universal crimper press (PerkinElmer, US). Along with the sample, an empty sample pan was sealed as a reference for the DSC measurements. The following compounds were used without any further purification: Me_2SO (WAK-Chemie Medical GmbH, Germany), ethylene glycol (Sigma-Aldrich Chemie GmbH, Germany) and a 50%/50% mixture of Me_2SO and EG. These compounds were added to PBS (Gibco, Thermo Fischer Scientific, Germany) in varying concentrations. We furthermore investigated an established vitrification medium (VS) consisting of 20 vol% Me_2SO, 20 vol% EG and 60 vol% hESC culture medium. The hESC medium is comprised of Dulbecco's modified eagle medium (DMEM F12; Gibco, Thermo Fischer Scientific, Germany), 0.1 mmol/l β-mercaptoethanol (Sigma–Aldrich Chemie GmbH, Germany), 20% syntactical serum replacer, 2 mmol/l L-glutamine, 1% non-essential amino acids, 4 ng/ml human recombinant bFGF, 100 U/ml penicillin, and 100 µg/ml streptomycin (all from Invitrogen, Germany). Finally, 300 mM sucrose (Sigma-Aldrich Chemie GmbH, Germany) was added to the medium.

2.2. DSC

In order to study devitrification kinetics isothermal DSC measurements were performed. Isothermal DSC measurements were chosen since they idealize a transient exposure to elevated temperatures best. Isothermal measurements are limited to the temperature range that leads to sample devitrification over a few minutes to hours for practical reasons. This is also the time regime relevant to most biobank procedures. Both the investigated sample as well as an empty reference sample were loaded into a DSC (DSC 8500, PerkinElmer, US), that measures the relative heat flow between the sample and reference when exposed to a given temperature protocol. The measured heat-flow is in comparison to the empty reference sample and a negative heat-flow therefore signifies an exothermic process, such as a crystallization. An example of a typical temperature protocol used for the isothermal measurements is shown in Fig. 1. The furnaces get in contact with a copper block that is pre-cooled to −160 °C allowing for a rapid ballistic cooling from 20 °C to −140 °C, which is well below T_g. The samples are

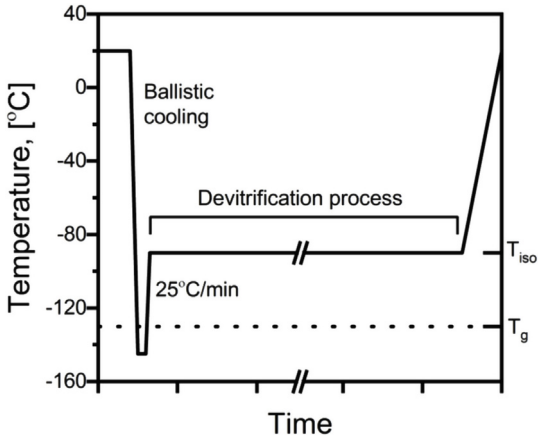

Fig. 1. Sketch of a typical temperature profile for the isothermal DSC-measurements. The sample is first rapidly cooled below T_g in order to vitrify the sample. Before heating to the isothermal temperature the sample is kept there for 5 min in order for the system to equilibrate. The sample is then heated at 25 K/min to T_{iso} where it is kept while the devitrification process takes place. The sample is finally heated to room temperature.

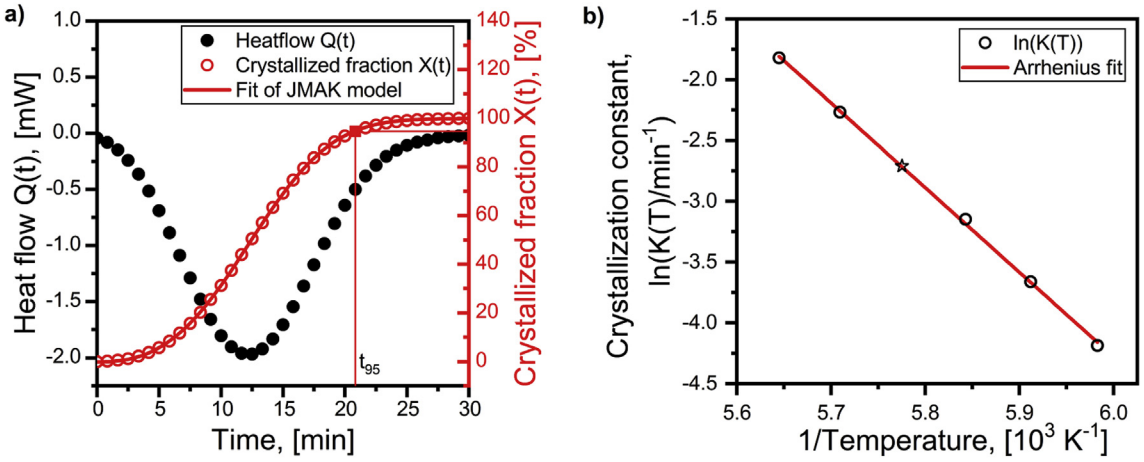

Fig. 2. a) A typical measurement of heat-flow at T_{iso}. The measurement shown is for the 49 wt% EG/Me_2SO mixture at −100 °C. Only 1 in 500 data points is shown. The heat-flow *Q(t)* is also converted to the fraction *X(t)* that has crystallized. The JMAK model has been fitted to *X(t)* in order to extract a crystallization constant of 0.067min^{-1}. The value for t_{95} is marked as a square. b) Arrhenius fit of crystallization constants determined for the 49 wt% EG/Me_2SO mixture. The Arrhenius fit revealed an E_A of 57.8 ± 0.7 kJ/mol and a $\ln(K_0/min^{-1})$ of 37.5 ± 0.5. The star marks the crystallization constant found in (a).

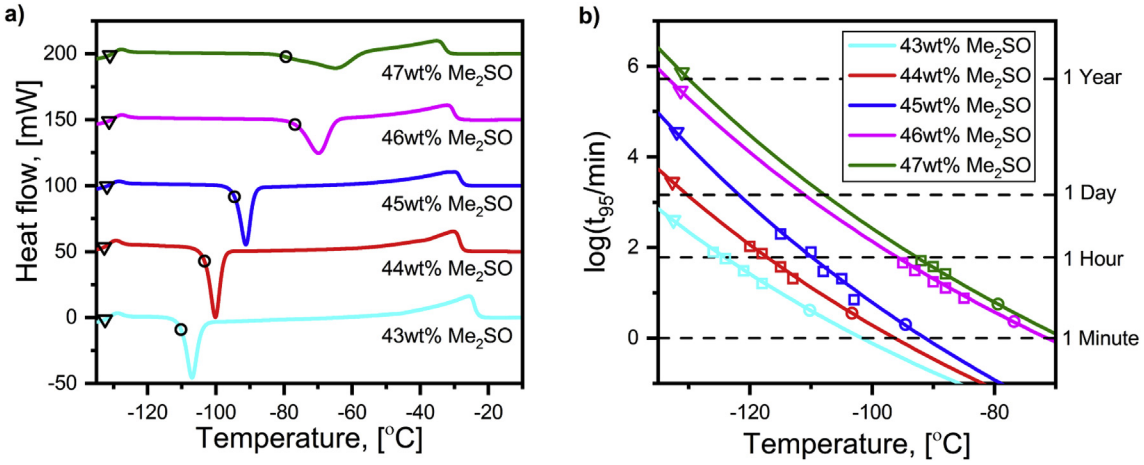

Fig. 3. a) T-sweep DSC measurements of mixtures containing Me_2SO at increasing concentrations. The heating-rate was 10 K/min. Herein the glass transition temperatures (triangles) and crystallization points (circles) are determined. b) Calculated devitrification times t_{95} based on measurement of the crystallization constant (lines) and measured values for t_{95} (squares). Glass transition temperatures (triangles) and crystallization temperatures (circles) at 10 K/min heating are also shown at the calculated t_{95}-lines.

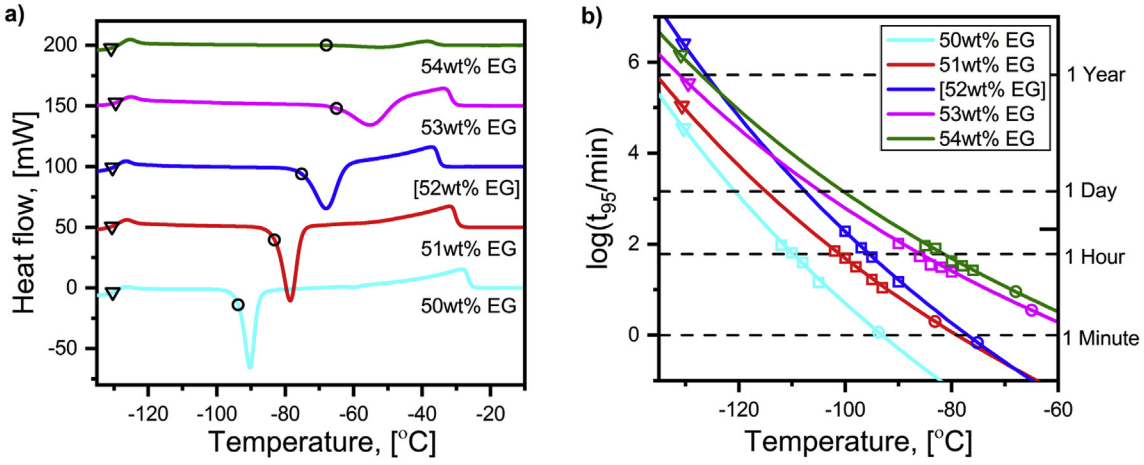

Fig. 4. a) T-sweep DSC measurements of mixtures containing EG at increasing concentrations. The heating-rate was 10 K/min. Herein the glass transition temperatures (triangles) and crystallization points (circles) are determined. b) Calculated devitrification times t_{95} based on measurement of the crystallization constant (lines) and measured values for t_{95} (squares). Glass transition temperatures (triangles) and crystallization temperatures (circles) at 10 K/min heating are also shown at the calculated t_{95}-lines. The data in brackets (52% T-sweep and t_{95}-plot) seem to be unsound due to a calibration error (see text).

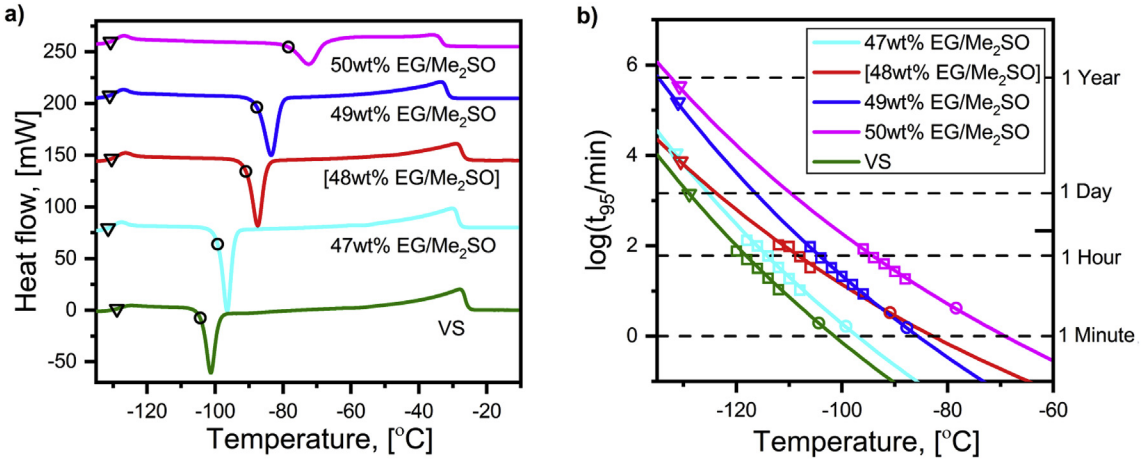

Fig. 5. a) T-sweep DSC measurements of samples containing EG/Me_2SO mixture at increasing concentrations and of the VS medium. The heating-rate was 10 K/min. Herein the glass transition temperatures (triangles) and crystallization points (circles) are determined. b) Calculated devitrification times t_{95} based on measurement of the crystallization constant (lines) and measured values for t_{95} (squares). Glass transition temperatures (triangles) and crystallization temperatures (circles) at 10 K/min heating are also shown at the calculated t_{95}-lines. The data in brackets (48% T-sweep and t_{95}-plot) seem to be unsound due to a calibration error (see text).

kept at −140 °C for 5 min before being heated at 25 K/min to the temperature that is being investigated, T_{iso}. The sample is kept at this temperature for a varying period in order for the devitrification process to complete. Finally, the sample is again heated to 20 °C before a new measurement is performed on the same sample but at different T_{iso}. The range of T_{iso} was determined by first performing a T-sweep scan with an unbroken heating of 10 K/min from −140 °C to 20 °C. Here a practical upper limit for T_{iso} can be determined since ice will start to crystallize at a given temperature. Measuring above this temperature will lead to devitrification times too short for proper analysis. In practice, a temperature range of approximately 10–15 K below the upper limit was feasible. When T_{iso} is too far from the upper limit, the crystallization process is stretched out over a very long period. So the heat flow curve flattens and becomes prone to noise and drift. The glass transition temperatures (triangles in Figs. 3a–5a) were graphically determined as 50%-rise-temperature and the crystallization points (circles in Figs. 3a–5a) were determined at the onset by graphical extrapolation.

2.3. Johnson-Mehl-Avrami-Kolmogorov (JMAK) model

The JMAK model describes crystallization phase transition kinetics in supercooled melts and glasses [1–3,17,19]. The fraction of ice X crystallized at time t under isothermal conditions can be described according to Ref. [40].

$$X(t) = 1 - \exp\left(-A\int_0^t I_v\left(\int_{t'}^t u\,dt\right)^m dt'\right) \tag{1}$$

Here I_v and u describes the ice nucleation and radial ice crystal growth rate, respectively. m depends on the dimensionality of the crystallization. Time-independent constants are collected in A. At the temperature T this can be rewritten to

$$X(t) = 1 - \exp(-(K(T)t)^n) \tag{2}$$

under the assumption that u and I_v are constant. Here $K(T)$ is a crystallization constant and n is related to m. We assume a 3D ice crystal growth and zero nucleation rate at the isothermal hold temperature [14]. This leads to exponents $n = m = 3$ for interface controlled growth and $n = m = 3/2$ for diffusion controlled growth [15]. Fits of our experimental data with variable n yields exponents closely around 3. The average exponent over all data is $n = 3.07 \pm 0.57$ Hence we used n fixed to 3 to treat all experimental data consistently. The crystallization constant $K(T)$ exhibits an Arrhenian temperature dependence over the observed temperature range:

$$K(T) = K_0\exp\left(-\frac{E_A}{RT}\right) \tag{3}$$

with E_A being the activation energy for the devitrification process. K_0 is a hypothetical constant describing the crystallization constant at infinite temperature, $K_0 = K(\infty)$. We define t_x as the time it takes for the fraction X of the devitrification process to occur:

$$t_x(T) = -\frac{\ln(1-X)^{1/n}}{K(T)} \tag{4}$$

We will arbitrarily use t_{95} as a measure for the devitrification duration:

$$t_{95}(T) = -\frac{\ln(0.05)^{1/n}}{K(T)} \tag{5}$$

During the crystallization process, we can assume that

$$\frac{dX(t)}{dt} \propto \mathrm{abs}(Q(t)), \tag{6}$$

where $Q(t)$ is the measured heat-flow. This means that we can estimate X(t) by calculating the sum

$$X(t) = \frac{\sum_{t=0}^{t} Q(t')}{\sum_{t=0}^{t_{end}} Q(t')} \tag{7}$$

We define t_{end} as the time where the devitrification process has completed and $Q(t) \approx 0$ mW. An example of a devitrification process is shown in Fig. 2a for a 49 wt% EG/Me_2SO mixture at −100 °C. Here both $Q(t)$ (black circles) and the calculated $X(t)$ (red circles) are shown. The crystallized fraction $X(t)$ data were fitted using the JMAK model to obtain the crystallization constant. The respective value for t_{95} is indicated as a square. We performed this at multiple temperatures, so that E_A and K_0 can be determined for this mixture as shown in Fig. 2b. The Arrhenius equation was transformed to a linear relation to ensure a robust fitting procedure. The crystallization constant determined in Fig. 2a is indicated with a star.

3. Results

We investigated three different mixtures consisting of Me_2SO, EG and EG/Me_2SO at varying concentrations as well as the vitrification medium VS. For each chemical composition at first a temperature sweep (T-sweep) DSC-measurement was performed to determine a

practical upper limit of the measurement, with subsequent isothermal measurements at three to seven different temperatures in order to determine $K(T)$.

The results for the Me_2SO mixtures are shown in Fig. 3. Five concentrations of Me_2SO in PBS were investigated: 43 wt%, 44 wt%, 45 wt %, 46 wt% and 47 wt%. Fig. 3a shows the T-sweep measurements where T_g (triangles) and crystallization temperature (circles) (at 10 K/min heating) have been graphically ascertained. We first of all observed that T_g increases only slightly from −132.5 °C to −131.1 °C when increasing the Me_2SO concentration from 43 wt% to 47 wt%, which was expected [26]. With increasing concentration the crystallization temperature increases dramatically, which is expected since higher concentrations of Me_2SO are known to more easily form a glass [36]. It should be noted that for the 47 wt% measurement the crystallization peak and melting peak seem to overlap which in turn results in a skewed crystallization peak and therefore a lower estimated crystallization temperature compared to the 46 wt% measurement. The crystallization peak is here stretched out and has a lower maximum value. The heating rate of 10 K/min was however kept so that all samples were treated equally. The melting temperature is seen to decrease with Me_2SO concentration as expected from the Me_2SO-H_2O phase diagram [29].

For each concentration a series of varying isothermal temperatures were performed yielding E_A and K_0. From this, t_{95} was calculated as a function of temperature and shown in Fig. 3b along with measured values for t_{95} (squares). If devitrification times for alternate crystalized fractions t_X were plotted, all curves would just be shifted vertically. The glass transition temperature (triangles) and crystallization temperature (circles) are also marked for each composition at their respective calculated t_{95}-curve. The devitrification kinetics have a strong dependence on the Me_2SO concentration. The higher the Me_2SO concentration the longer it takes the glass to devitrify at the same temperature and is thus a more stable glass. For a concentration of 43 wt% Me_2SO it takes 1 h for the glass to devitrify at approximately −125 °C. For a mixture with 47 wt% Me_2SO this first happen at approximately −92 °C. This is a significant temperature range and a 47 wt% Me_2SO mixture is hence dramatically less sensitive to slight temperature elevations above T_g.

The T-sweep DSC-measurements for the EG-mixtures are shown in Fig. 4a. Here we investigated the following concentrations: 50 wt%, 51 wt%, 52 wt%, 53 wt% and 54 wt%. Even though EG has a higher eutectic temperature compared to Me_2SO [8] we still see an overlap between the crystallization and melting peak for the mixtures containing more than 53 wt% EG. This results in the same skewing of the crystallization peak as with Me_2SO. In post-processing of our data we noticed that the peak temperature of melting of the 52 wt% sample seem to be lower than expected compared to the other samples. Presumably, an error occurred in the experimental procedure for this particular sample that lead to a mismatch in the temperature scale. We will later discuss the consequences of mismatch in the temperature scale and have therefore kept the data in the figures.

The calculated t_{95}-curves based on $K(T)$ are shown in Fig. 4b along with the measured t_{95}-data points. Here we see the same trends as with Me_2SO, i.e. a strong dependence of devitrification times on EG concentration. A devitrification time of 1 h spans a temperature range of −110 °C to −80 °C for the investigated EG concentrations. The measurements done on the 52 wt% EG sample does however have a significantly different slope compared to the other EG-concentrations. All measurements for 52 wt% EG are performed on a single sample and seem consistent over the measured temperature range. We can exclude errors in the mixture preparation, since this would effectively shift the curve towards either the 51 wt% or 53 wt% curve but maintaining the correct slope. We instead believe that the nucleation of this particular sample in some fashion has been impacted increasing the temperature sensitivity or that some error has occurred in the experimental procedure as previously mentioned.

Fig. 5 contains the measurements of the 50%/50% EG/Me_2SO mixtures as well as for the VS medium. We investigated the following concentrations of the EG/Me_2SO mixtures: 47 wt%, 48 wt%, 49 wt% and 50 wt%. The T-sweep measurements are shown in Fig. 5a. As with the other investigated mixtures the crystallization point of the EG/Me_2SO mixture is seen to increase with concentration. The increase does however seem to be less dependent on CPA concentration as compared to the pure Me_2SO and EG mixtures. Here a concentration change of 3 wt% results in a crystallization temperature change of about 20 K compared to 25–30 K for the pure compounds. Again an overlap between the crystallization and melting peak is observed for the highest concentration investigated (50 wt%). The VS medium is found to have a slightly lower crystallization temperature of −104 °C compared to −99 °C of 47 wt% EG/Me_2SO. This should be seen in the light of VS only containing 38.5 wt% EG/Me_2SO. If the sample would not contain sucrose we would have expected a crystallization temperature significantly lower than that of 47 wt% EG/Me_2SO. We also observed that T_g of the VS medium is slightly higher ($T_g \approx -129$ °C) than for the EG/Me_2SO mixtures ($T_g \approx -131$ °C).

Fig. 5b contains the calculated (line) and measured values (squares) for t_{95}. Here we find that the temperature required for an 1 h devitrification time spans from approximately −115 °C to −95 °C for the measured concentrations of the EG/Me_2SO mixture. This is a slightly shorter range than for the pure Me_2SO and EG mixtures. This also holds true when taking into account that for this mixture a concentration range over only 3 wt% was investigated compared to the 4 wt% range of the other mixtures. We furthermore observe that the measurements of the 48 wt% EG/Me_2SO mixture does not align with the other concentrations. This deviation could be attributed the measurement performed at −112 °C where the measured t_{95} seems to be an outlier. In effect this reduces $K(-112°C)$ and therefore also E_A for this particular mixture. We did however also observe that the melting peak in the T-sweep is located at a higher temperature than the neighboring sample, which could be an indication of an error in the experimental procedure comparable to that of the 52 wt% EG sample. Finally we observe that the VS medium seem to devitrify faster than the other EG/Me_2SO mixtures, which was expected due to the lower content of EG and Me_2SO. The decrease in devitrification times are however small when compared to the 47 wt% EG/Me_2SO mixture, due to the additional content of sucrose in this medium.

Table 1 contains values for E_A, K_0 and t_{95}(-100 °C) yielded by the JMAK model for the isothermal DSC measurements. It was previously mentioned that the measurements for the 52 wt% EG and 48 wt% EG/Me_2SO mixtures deviate from the other measurements and seem to be erroneous. The 48 wt% EG/Me_2SO has also the highest standard deviation of the EG/Me_2SO mixtures, which is an effect of the erroneous $K(-112°C)$ measurement. The values for t_{95}(-100 °C) shows that already small concentration changes have a profound impact on the devitrification kinetics. Finally, we have estimated the amount of water crystallized in a given sample (as the percentage of absolute sample weight Q_{H2O}) by integrating the crystallization peak in the T-Sweep DSC measurement. It is safe to assume that we only see water crystallizing in our experiments since we did not see eutectic melting in any of the DSC measurements, which would have shown up as an endothermic peak at the eutectic temperature (around −70 °C for Me_2SO and around −50 °C for EG). We have used the heat of fusion for pure water (and ideal mixtures) $\Delta H_F = 334$ J/g to simplify matters. Certainly, aqueous mixtures of Me_2SO, EG and electrolytes are far from being ideal and excess mixing heat will vary ΔH_F of our samples to a certain extent. From here, an absolute increase in the CPA concentration in the non-crystallized fraction of the sample can be roughly calculated:

$$\Delta[\mathrm{CPA}] = [\mathrm{CPA}]_{\mathrm{end}} - [\mathrm{CPA}]_0$$

We found that the CPA concentration during devitrification increased between 3 wt% and 7 wt% depending on the sample composition. For the VS medium the absolute increase for both the EG/Me_2SO and sucrose has been calculated.

Table 1
The E_A and K_0 for the investigated mixtures yielded from the isothermal measurements. The calculated t_{95}(-100 °C) are also shown. From the T-Sweep measurements we have estimated the amount of crystallized H_2O (Q_{H2O}) and calculated the absolute increase of CPA-concentration ($\Delta[CPA]$, as the fraction of the total sample weight). For the VS medium $\Delta[CPA]$ gives the increase in EG/Me_2SO and sucrose, respectively.

Concentration	E_A/kJ mol^{-1}	ln(K_0/min^{-1})	t_{95}(-100 °C)/min	Q_{H2O}/wt%	Δ[CPA]/wt%
43 wt% Me_2SO	38.8 ± 1.4	27.6 ± 1.1	0.77	7.0	3.2
44 wt% Me_2SO	41.8 ± 4.6	28.7 ± 3.5	1.92	7.4	3.5
45 wt% Me_2SO	54.6 ± 7.1	36.5 ± 5.2	6.13	6.6	3.5
46 wt% Me_2SO	49.9 ± 0.9	30.1 ± 0.6	136.0	NA	NA
47 wt% Me_2SO	52.1 ± 9.2	31.0 ± 6.0	263.4	NA	NA
50 wt% EG	59.9 ± 6.9	40.4 ± 5.0	5.00	10.0	5.5
51 wt% EG	51.6 ± 2.4	32.3 ± 1.6	48.80	12.0	6.9
[52 wt% EG]	[64.2 ± 1.1]	[39.7 ± 0.7]	[188.4]	[NA]	[NA]
53 wt% EG	44.1 ± 1.5	24.6 ± 1.0	620.6	NA	NA
54 wt% EG	46.1 ± 5.9	25.2 ± 3.7	1352.7	NA	NA
47 wt% EG/Me_2SO	55.9 ± 3.9	38.5 ± 3.0	1.88	10.2	5.3
[48 wt% EG/Me_2SO]	[42.0 ± 7.9]	[26.9 ± 5.7]	[13.99]	9.7	[5.1]
49 wt% EG/Me_2SO	57.9 ± 0.7	37.5 ± 0.5	21.78	NA	NA
50 wt% EG/Me_2SO	49.7 ± 1.9	29.6 ± 1.3	186.1	NA	NA
VS medium	54.3 ± 2.4	38.4 ± 1.8	0.73	7.8	3.3/0.7

4. Discussion

The JMAK model seems to be appropriate to describe our data. An example hereof is the fit of the model in Fig. 2 as well as the Arrhenius dependence of the crystallization constant. By applying the JMAK model on such DSC measurements it is possible to compare different vitrification media and determine its sensitivity to temperature elevations above T_g. According to Ref. [17], a deviation from the symmetrical, sigmoidal shape of equation (2) only occurs, if the product $I_V \times u^3$ (which is implied in K) is not constant during the devitrification process. Since we find our data to agree with equation (2), either changes of I_V and u^3 compensate each other for all compositions and temperatures (very unlikely) or both I_V and u^3 do not change noticeably during isothermal devitrification. Due to u being cubed, this kind of examination is much more sensitive to changes in growth rate u than it is in nucleation rate I_V. During devitrification, water will crystallize in the sample. Hence the overall CPA concentration in the non-crystallized part of the sample increases, which in turn will increase the viscosity of the non-crystalized fraction [32,41] and decrease the concentration of available H_2O for further crystal growth. Since the JMAK model fits our data we can deduce that the dependence of CPA-concentration on the ice crystal growth u is negligible compared to its dependence on temperature. The JMAK model assumes that u remains constant during devitrification. If u changes during the devitrification due to a CPA content increase, a slowdown of ice crystallization will occur and the process will noticeably deviate from the JMAK model [17]. The increase in CPA concentration in the non-crystalized fraction during devitrification is comparable to or even bigger than the range of initial CPA concentrations investigated. We however observed that the initial CPA concentration has a significant impact on devitrification rate. Combining this observation with the independence of crystal growth rate on CPA concentration in the non-crystalized fraction, we can conclude that the strong dependence of the devitrification times on initial CPA concentration is the mainly caused by an alteration of the nucleation rate.

For Me_2SO it is safe to assume that the nucleation rate is zero at temperatures above −104 °C according to Refs. [14,15]. But the data obtained at lower isothermal hold temperatures down to −120 °C agree with an exponent $n = 3$, too, which is consistent to a growth-dominated devitrification. A significant peak of the nucleation rate in aqueous Me_2SO solutions was found closely around the glass transition at about −130 °C [14], that rapidly declines with temperature. Hence, the temperature dependence observed in the devitrification kinetics above −120 °C predominantly originates from the ice crystal growth rate. The nucleation rate in the sample is similarly only dependent on the initial CPA concentration. Here the nuclei present are either heterogeneously formed or are conserved nuclei formed homogeneously during the cooling, thermal hold and subsequent heating to the isothermal observation temperature in accordance to the study by Hey et al. [14]. For EG and EG/Me_2SO mixtures there is no information from literature about the nucleation rate and it is possible that ice nuclei form during the devitrification process. The shape of the devitrification curve will remain the same even if the number of nuclei is changing at a constant rate [17]. However, the exponent n being close to 3 indicates a growth-dominated devitrification for these two mixtures, too. We therefore cannot distinguish between a temperature dependence due to crystal growth rate or due to nucleation rate here. For these two types of mixtures, we can however still conclude that the initial CPA concentration is influencing primarily the nucleation part of the devitrification.

We have argued that the change in crystal growth rate upon changes in CPA concentration of the non-crystallized fraction during devitrification is negligible, which is in line with an earlier study that used transmission microscopy to show constant ice crystal growth rates within a short time frame (< 1 min) for a 45 wt% Me_2SO mixture [16]. Since devitrification not only concentrates solutes in the non-crystallized fraction, but also forms water concentration gradients above the ice surface due to the inclusion of water into the crystal lattice, viscosity and diffusivity of the non-crystalized fraction should vary during the devitrification process. The almost constant crystal growth hence indicates that the devitrification kinetics are predominantly interface controlled as opposed to diffusion controlled. This is supported by JMAK fits with variable n that yields a mean $n = 3.07 \pm 0.57$ across all measurements. For diffusion-controlled kinetics we would expect n close to 3/2.

Let us now consider the investigations on Me_2SO and EG. Lower concentrations of Me_2SO are required to obtain the same $t_{95}(T)$ when compared to EG, which was expected since Me_2SO is a stronger glass former [4,26] and strong glass formers are less likely to devitrify. Another point where we can compare Me_2SO to EG is their sensitivity to changes in initial CPA-concentration. When changing the initial Me_2SO concentration by 4 wt% the t_{95}(-100 °C) changes by a factor of 342 compared to a factor of 271 for EG. This means that the devitrification stability depends stronger on CPA-concentration for Me_2SO solutions than for EG solutions. This is not necessary to the detriment of the usability of Me_2SO, since a higher sensitivity allow for an easier manipulation of the physical properties of a vitrification medium. Me_2SO is thus the better choice as a CPA compared to EG when only taking the stability of the vitrified state into consideration. Other aspects such as cytotoxicity have to be considered, too, in the development of new cryopreservation media. Extended periods of high Me_2SO exposure are unwanted due to cytotoxicity. In this aspect higher sensitivity to initial

concentration is a good characteristic since it allows for a stronger manipulation with only low impact on the cytotoxicity. Our data show that even small increases in initial CPA concentration significantly increase the stability of the vitrified state.

The concentrations of EG/Me_2SO required to obtain comparable devitrification times as observed for pure Me_2SO and EG samples are in-between those of the Me_2SO and EG samples, which was to be expected taking the composition of the mixture into account. A surprising finding was that the concentration dependence was lower than that of both pure Me_2SO and EG solutions. A change by 3 wt% was found to change t_{95}(-100 °C) by a factor of 99, compared to 177 and 124 for pure Me_2SO and EG respectively. This lower sensitivity here is attributed to both EG and Me_2SO concentrations being far away from compositions where hydrates of the CPAs can form (at molar ratios of 1:2 and 1:3 for Me_2SO, 1:1 for EG).

A comparison of the concentration dependency of the parameters E_A and K_0 for Me_2SO and EG (see Table 1) shows converse tendencies: For Me_2SO we find increasing E_A and declining K_0 on ascending CPA concentration, while for EG the situation is opposed. The absolute value of E_A = 54,6 kJ/mol for 45% Me_2SO in this work is about 60% higher than the corresponding values given in the work of Hey et al. [15]. We attribute this deviation to the different composition of the samples. Whereas Hey et al. use distilled water in their mixtures, we investigated mixtures with phosphate-buffered saline (PBS). This cell culture product contains about 155 mM NaCl and a total of 3 mM phosphates (in different protonation levels). Solvated electrolytes disturb the molecular order of water significantly and may have serious effects on the growth rate of ice crystals.

The VS medium has the shortest devitrification times of all the investigated mixtures (Fig. 5), which can be attributed to the relatively low CPA concentrations. The medium is hence comparably unstable above T_g and even short temperature elevations can prove detrimental to the sample. This raises the question of why such media are employed in state of the art cryopreservation protocols. The answer is that the obstacle of successfully persevering very sensitive cell types as well lies in the biocompatibility of the preservation medium and not only in the ability to rapidly cool and rewarm a sample. For the VS medium Me_2SO and EG are partly replaced by sucrose to maintain the glass forming tendency of the medium while reducing the cytotoxic effects of Me_2SO and EG. This poses a tradeoff between stability of the vitrified state and lower cytotoxic effects. When the cooling and rewarming processes are thoroughly optimized, any further improvements of the cryopreservation process would have to originate from medium optimizations. This requires good standards in terms of cooling, handling and rewarming protocols to ensure that unwanted devitrification is avoided.

The data presented in this work mirrors the requirements of the cooling/heating rate for a successful vitrification and subsequent rewarming. A mixture with higher CPA concentration is less sensitive to temperature elevations above T_g and it is thus more unlikely that devitrification will occur. This also holds true during the initial vitrification and final rewarming of the sample, and a lower cooling/heating rate can be employed to achieve a successful preservation through vitrification. This means that a mixture with a slightly higher CPA concentration does not only pose less requirements to the vitrification and rewarming process, it is also more insensitive to temperature elevations above T_g.

Concerning the practical use of the described experimental protocol it is very appealing that two medium-specific measures (K_0 and E_A) allow to calculate maximum exposure times for a given temperature in an easy manner instead of extracting them from a time-temperature-transition (TTT) chart (that would yet have to be set up for each medium composition). In fact, the stability plots (Figs. 3b–5b) are comparable to sections of TTT-charts with interchanged axes. The extrapolation of the devitrification times t_X towards T_g and towards the melting temperature is not strictly valid, since one cannot assume a stringent Arrhenian behavior over wide temperature ranges. The devitrification rate reflects several temperature-dependent properties of the supercooled liquid, including viscosity and homogeneous nucleation tendency. For Me_2SO the homogeneous nucleation rate was found to have a narrow maximum around T_g [14,39], a clearly non-Arrhenian behavior. The viscosity of glass-forming liquids behaves Arrhenian only apart from T_g and over limited temperature ranges. It is often described by the Vogel-Fulcher-Tammann (VFT) model instead of the Arrhenius equation [39]. The VFT model uses the difference to a material-specific temperature (mostly close to T_g) as variable, not the absolute temperature. However, the results will still be very useful approximations in the temperature and time regimes of biobank sample handling.

Unlike the idealized isothermal conditions assumed in our experiment, exposing a sample to an atmosphere of elevated temperature will lead to slow sample heating until the ambient temperature is attained. The calculated maximum exposure times will therefore always be worst-case-scenario values.

The execution of the measurement of this protocol might be slightly more time-consuming compared to non-isothermal techniques, but easy to conduct, easy to analyze and without assumptions required for non-isothermal data analysis [12,15]. How experimental errors influence the outcome can be nicely seen at the 52% EG medium and the 48% EG/Me_2SO medium. Here, implausible slopes of the stability function coincide with conspicuous deviations of the T-sweep curves. Most likely, the experimental parameters (e.g. purge gas flow in the DSC) were off the values used in the temperature calibration. We do however see that the measured t_{95} values are within the expected range compared to the other measurements. That means that we can still use these measurements to estimate the glass stability of the given samples. In these cases, it is however not recommendable to extensively extrapolate the results beyond the measured temperature range.

Beyond the assessment of medium stability against devitrification for proper sample handling, the investigated dependence of K_0 and E_A on CPA concentration is very useful. Knowing such trends for different CPA and their combinations can help in the trade-off between devitrification stability and specimen toxicity in the composition of new vitrification media.

4.1. A general protocol for determination of K_0, E_A and their use

In order to enable researchers without a background in thermodynamics and chemical kinetics to conduct a determination of the ice formation activation energy E_A and the medium-specific constant K_0 for the assessment of critical times at elevated temperatures in sample handling, we present a protocol including the essential steps. It is written in a general way, so the protocol may be implemented on DSC instruments of different manufacturers as well as using different data analysis tools. One could even think of yielding the crystallization kinetics data using unorthodox experimental setups like Raman spectroscopy [10] (In contrast to DSC, where $Q(t)$ is recorded, Raman spectroscopy probes $X(t)$ directly).

1) Identification of an appropriate sample volume: In order to use the available heat scale of your DSC, put some ten µL pure water into a sample pan and perform a T-sweep with $dT/dt = -10$ K/min against an empty pan. Adjust the sample volume in a way that the exothermic crystallization peak just matches the maximum heat scale of your instrument. At identical sample volume, all aqueous mixtures will show smaller exothermic amplitudes. If you like to determine the equilibrium melting temperatures of your mixtures, too, you need to carry out a heating T-sweep scan of the chosen volume of pure water at +10 K/min. This will yield the required slope for graphical analysis.
2) Identification of the useful temperature range for isothermal experiments: This has to be performed for each medium composition. Fill in the volume determined under (1) into a sample pan. Load your DSC with your sample pan and an empty pan as reference.

Vitrify your sample by ballistic cooling (uncontrolled as-fast-as-possible cooling) down to −140 °C or lower. Perform a T-sweep scan from −140 °C up to 20 °C at $dT/dt = +10$ K/min. If your vitrification was successful, your DSC-scan will show (a) a glass transition around −130 °C, (b) an exothermic devitrification peak between the glass transition and the eutectic and (c) a broad endothermic melting process starting at the eutectic up to the mixtures melting temperature. The upper temperature limit for isothermal scans is the onset temperature of devitrification (by graphical analysis: at the intersection of the extrapolated baseline and the tangent to the low temperature inflection point of the devitrification peak). Start you isothermal scans at that temperature and step down −3 K for the next one. These are your isothermal scan temperatures T_{iso}. Repeat this until the exothermic devitrification peaks are too stretched-out for a proper data fitting (approximately −10 K to −15 K below your upper limit). If you do not observe a glass transition and a devitrification, vitrification was unsuccessful. If you observe a glass transition, but neither devitrification nor melting, your medium is extraordinarily stable against devitrification. We observed such behavior only for mixtures with water content much lower than 50%, which is assumably too low for vital specimens.

3) Isothermal scans: Proceed with the sample from (2) at a time. Vitrify the sample by ballistic cooling down to −140 °C again and hold them at −140 °C for 5 min. Heat your sample to the isothermal scan temperature T_{iso} at +25 K/min. Now keep the temperature constant and record the heat flux $Q(t)$ until the devitrification has completed. Heat your sample to room temperature and repeat the experiment with the next lower T_{iso}.
4) Import the heat flux data $Q(t)$ of your isothermal scans into a data analysis software, subtract any background and convert them to crystalized fraction data $X(t)$ using equation (7) (If your data comes from Raman spectroscopy or other techniques that directly probe the crystallized fraction $X(t)$, just subtract the background and normalize the data).
5) Now let the data analysis software fit equation (2) to your crystalized fraction data $X(t)$. Set the exponent n to 3 (fixed). This will yield the crystallization constant $K(T)$ for a given temperature (and mixture).
6) Next, plot the logarithm of your crystallization constants $\ln[K(T)]$ against the reciprocal temperature $1/T$ (in Kelvin) in an Arrhenius chart. A linear fit to the plot will yield you the activation energy E_A as the slope $-E_A/R$ and the specific constant K_0 as the ordinate intercept $\ln K_0$.
7) Having E_A and K_0 allows you to assess $K(T)$ over a wide temperature range from the glass transition to the eutectic by the Arrhenian equation (3). Using $K(T)$ in equation (4) (with the exponent fixed to $n = 3$) leads to the time it takes for the crystallization of a given fraction X at elevated temperature. Please note, that the crystallized fraction refers to the maximum amount of water that crystallizes in a devitrification process under the given conditions (see Table 1), not to the total amount of water in the sample.
8) Some remarks on the application: If you accept a certain crystallized fraction X of your sample to be safe, remember that devitrification is irreversible. Next time you elevate the temperature of your sample above the glass transition temperature, devitrification will not start at $X = 0$, but proceed from the fraction X, that was crystallized before.
9) The calculated crystallization times are worst-case scenarios. In daily life sample handling, you will expose your samples to an atmosphere of elevated temperature for a limited time. The payload of your sample container will yet heat up much slower, since the heat transfer from the gas phase to a condensed sample is low.
10) You may now include the calculated crystallization times into your sample handling protocols in order to avoid harmful temperature exposure (in terms of maximum exposure duration and iterations).

5. Conclusion

We have here studied the devitrification kinetics of common CPAs using DSC and investigated the effect of changing the CPA concentration. We found that slight changes in CPA concentration have a significant impact on the devitrification kinetics. The devitrification kinetics have successfully been modelled by the JMAK model, which allows to predict the devitrification kinetics in the proximity of the investigated temperature range. We found that Me_2SO are more sensitive to changes in concentration compared to EG.

We have shown that using too low CPA concentrations in a vitrification medium makes a sample very sensitive to slight temperature elevations above T_g. It is however possible to increase the stability of the sample, where small increases in CPA concentrations can make the samples about 100-fold more robust against devitrification. Stability of the vitrified state could be included in the development of new cryopreservation protocols, since only small changes in CPA concentrations are required for a significant effect.

The method proved to be an easy to conduct protocol to yield two medium-specific values, K_0 and E_A, which allow calculating maximum exposure times for the given medium at relevant temperatures.

Declaration of interests

The authors declare no conflict of interests.

References

[1] M. Avrami, Kinetics of phase change. I general theory, J. Chem. Phys. 7 (1939) 1103–1112.
[2] M. Avrami, Kinetics of phase change. II transformation-time relations for random distribution of nuclei, J. Chem. Phys. 8 (1940) 212–224.
[3] M. Avrami, Granulation, phase change, and microstructure kinetics of phase change. III, J. Chem. Phys. 9 (1941) 177–184.
[4] A. Baudot, L. Alger, P. Boutron, Glass-forming tendency in the system water-dimethyl sulfoxide, Cryobiology 40 (2000) 151–158.
[5] A.F. Beier, J.C. Schulz, H. Zimmermann, Cryopreservation with a twist - towards a sterile, serum-free surface-based vitrification of hESCs, Cryobiology 66 (2013) 8–16.
[6] P. Boutron, Comparison with the theory of the kinetics and extent of ice crystallization and of the glass-forming tendency in aqueous cryoprotective solutions, Cryobiology 23 (1986) 88–102.
[7] J.K. Choi, R. El Assal, N. Ng, E. Ginsburg, R.L. Maas, R.M. Anchan, U. Demirci, Bio-inspired solute enables preservation of human oocytes using minimum volume vitrification, J. Tissue Eng. Regenerat. Med. (2017) 1–8.
[8] D.R. Cordray, L.R. Kaplan, P.M. Woyciesjes, T.F. Kozak, Solid - liquid phase diagram for ethylene glycol + water, Fluid Phase Equilib. 117 (1996) 146–152.
[9] P.G. Debenedetti, H. Stillinger Frank, Supercooled liquids and the glass transition, Nature 410 (2001) 259–267.
[10] D. Dörr, F. Stracke, H. Zimmermann, Noninvasive quality control of cryopreserved samples, Biopreserv. Biobanking 10 (2012) 529–531.
[11] G.M. Fahy, D.R. Macfarlane, C.A. Angell, H.T. Meryman, Vitrification as an approach to cryopreservation, Cryobiology 21 (1984) 407–426.
[12] J. Farjas, P. Roura, Modification of the Kolmogorov-Johnson-Mehl-Avrami rate equation for non-isothermal experiments and its analytical solution, Acta Mater. 54 (2006) 5573–5579.
[13] A. Germann, Y.J. Oh, T. Schmidt, U. Schön, H. Zimmermann, H. von Briesen, Temperature fluctuations during deep temperature cryopreservation reduce PBMC recovery, viability and T-cell function, Cryobiology 67 (2013) 193–200.
[14] J.M. Hey, D.R. MacFarlane, Crystallization of ice in aqueous solutions of glycerol and dimethyl sulfoxide 1. A comparison of mechanisms, Cryobiology 33 (1996) 205–216.
[15] J.M. Hey, D.R. MacFarlane, Kinetic analyses of crystallization and devitrification: comparison of activation energies in aqueous solutions of glycerol and dimethyl sulphoxide, J. Non-Cryst. Solids 211 (1997) 262–270.
[16] J.M. Hey, D.R. MacFarlane, Crystallization of ice in aqueous solutions of glycerol and dimethyl sulfoxide 2: ice crystal growth kinetics, Cryobiology 37 (1998) 119–130.
[17] W.A. Johnson, R.F. Mehl, Reaction kinetics in processes of nucleation and growth, Trans. Am. Inst. Min. Metall. Eng. 135 (1939) 416–458.
[18] J.O.M. Karlsson, A theoretical model of intracellular devitrification, Cryobiology 42 (2001) 154–169.
[19] A. Kolmogorov, On the statistical theory of crystallization of metals [in Russian], Izv. Akad. Nauk SSSR Ser. Mat. 1 (1937) 355–359.
[20] M. Kuwayama, Highly efficient vitrification for cryopreservation of human oocytes and embryos: the Cryotop method, Theriogenology 67 (2007) 73–80.
[21] M. Lane, D.K. Gardner, Vitrification of mouse oocytes using a nylon loop, Mol.

Reprod. Dev. 58 (2001) 342–347.
[22] D.R. Macfarlane, Devitrification in glass-forming aqueous solutions, Cryobiology 23 (1986) 230–244.
[23] D.R. Macfarlane, Physical aspects of vitrification in aqueous solutions, Cryobiology 24 (1987) 181–195.
[24] P. Mazur, S. Seki, Survival of mouse oocytes after being cooled in a vitrification solution to -196°C at 95° to 70,000°C/min and warmed at 610° to 118,000°C/min: a new paradigm for cryopreservation by vitrification, Cryobiology 62 (2011) 1–7.
[25] P. Mehl, Isothermal and non-isothermal crystallization during warming in aqueous solutions of 1,3-butanediol: comparison of calorimetry and cryomicroscopy, Thermochim. Acta 155 (1989) 187–202.
[26] S.S.N. Murthy, Some insight into the physical basis of the cryoprotective action of dimethyl sulfoxide and ethylene glycol, Cryobiology 36 (1998) 84–96.
[27] J.C. Neubauer, A.F. Beier, N. Geijsen, H. Zimmermann, Cryopreservation and Freeze-Drying Protocols, Springer Science, 2015.
[28] W.F. Rall, G.M. Fahy, Ice-free cryopreservation of mouse embryos at −196 °C by vitrification, Nature 313 (1985) 573–575.
[29] D.H. Rasmussen, A.P. MacKenzie, Phase diagram for the system water–-dimethylsulphoxide, Nature 220 (1968) 1315–1317.
[30] B.E. Reubinoff, M.F. Pera, G. Vajta, A.O. Trounson, Effective cryopreservation of human embryonic stem cells by the open pulled straw vitrification method, Hum. Reprod. 16 (2001) 2187–2194.
[31] M. Richards, C.-Y. Fong, S. Tan, W.-K. Chan, A. Bongso, An efficient and safe xeno-free cryopreservation method for the storage of human embryonic stem cells, Stem Cell. 22 (2004) 779–789.
[32] S.A. Schichman, R.L. Amey, Viscosity and local liquid structure in dimethyl sulfoxide-water mixtures, J. Phys. Chem. 75 (1971) 98–102.
[33] S. Seki, P. Mazur, Kinetics and activation energy of recrystallization of intracellular ice in mouse oocytes subjected to interrupted rapid cooling, Cryobiology 56 (2008) 171–180.
[34] S. Seki, P. Mazur, The dominance of warming rate over cooling rate in the survival of mouse oocytes subjected to a vitrification procedure, Cryobiology 59 (2009) 75–82.
[35] S. Seki, P. Mazur, Ultra-rapid warming yields high survival of mouse oocytes cooled to -196°C in dilutions of a standard vitrification solution, PLoS One 7 (2012) 1–9.
[36] R.L. Sutton, Critical cooling rates to avoid ice crystallization in solutions of cryo-protective agents, J. Chem. Soc. Faraday. Trans. 87 (1991) 101–105.
[37] D.R. Uhlmann, A kinetic treatment of glass formation, J. Non-Cryst. Solids 7 (1972) 337–348.
[38] G. Vajta, P. Holm, M. Kuwayama, P.J. Booth, H. Jacobsen, T. Greve, H. Callesen, Open pulled straw (OPS) vitrification: a new way to reduce cryoinjuries of bovine ova and embryos, Mol. Reprod. Dev. 51 (1998) 53–58.
[39] B. Wowk, Thermodynamic aspects of vitrification, Cryobiology 60 (2010) 11–22.
[40] H. Yinnon, D.R. Uhlmann, Applications of thermoanalytical techniques to the study of crystallization kinetics in glass-forming liquids, part I: Theory, J. Non-Cryst. Solids 54 (1983) 253–275.
[41] S. Zhang, X. Yu, Z. Chen, G. Chen, Viscosities of the ternary solution dimethyl sulfoxide/water/sodium chloride at subzero temperatures and their application in cryopreservation, Cryobiology 66 (2013) 186–191.
[42] H. Zimmermann, A.D. Katsen, F.R. Ihmig, C.H.P. Durst, S.G. Shirley, G.R. Fuhr, First steps of an interdisciplinary approach towards miniaturised cryopreservation for cellular nanobiotechnology, IEE Proc. - Nanobiotechnol. 151 (2004) 134–138.